G. COMTE-BELLOT
Maître de Conférences.

A. STROHL
Chercheur 3 éme cycle.

E. ALCARAZ
Maître-Assistant.

Laboratoire de Mécanique des Fluides,
Ecole Centrale de Lyon,
69-Ecully, France

# On Aerodynamic Disturbances Caused by Single Hot-Wire Probes

*The disturbances which result from the different parts of single hot-wire probes (stem, prongs, wire sheath if any) are experimentally investigated by means of an auxiliary "reference" probe and are compared with evaluations derived from a potential flow scheme. Our findings suggest that the disturbances created by the prongs are usually 2–4 times greater than that produced by the stem, and that the wire sheath has a negligible effect. The global disturbance, closely equalling the sum of the separate ones, shows up as a velocity decrease when the probe is aligned with the mean flow (8 percent or less depending on the probe's geometry) and shows up as a velocity increase when the probe is normal to the mean flow (11 percent or less, again depending on the probe's geometry).*

## Introduction

Because of the relatively small size of its sensitive part, a hot-wire anemometer is generally considered to be a very convenient device for local velocity measurements in small spaces. However, the hot wire is part of a probe, and independent researchers have noticed that the measurements are noticeably affected not only by the probe configuration [1, 2][1] but are, more specifically dependent upon the manner in which the configurations are, in turn, oriented by the probe axis to the flow, the wire itself being kept normal to the flow [3–12].

By plotting the response detected by an anemometer Hoole and Calvert [5] appear to have been the first to quantitatively discern that the angle between the mean flow direction and the probe axis is an important parameter in the generation of perturbations. In more specific terms, a Disa 55-A-25 probe indicates a 20 percent higher velocity reading when its axis is rotated toward 90 deg than when its axis is fixed in a position near 0 deg. Gilmore [8] and later Dahm and Rasmussen [11] undertook more detailed investigations of the aerodynamic perturbation caused by probes. The former used a 10-times full-scale model of a probe, with removable prongs, while the latter, Dahm and Rasmussen, set, on given stems, prongs of varying diameters, lengths, and spacings. However, their results were still more or less general, for the reason that the same probe which acted as a measuring element, also, acted as a perturbating one.

In disagreement with the hypothesis presented by these authors, Eyre [6] and van Thinh [7] interpreted that changes in prong temperature due to different rates of cooling could account for measurement discrepancies. This interpretation seems questionable for two reasons: First, it is not quite consistent with the accurate wire temperature profiles obtained by Champagne, Sleicher, and Wehrmann [13], and second, the direction effect has been observed by Mathieu and his collaborators, even in cases in which a wollaston sheath covered both sides of the etched part of the wire.

The first objective of the present investigation was to assure that the aerodynamic perturbation caused by the probe was the most relevant factor, and the second was to separate and measure the perturbations coming from the different parts of a probe, i.e., from the stem, the prongs, and the wollaston sheath if any. In order to achieve these objectives an auxiliary probe was used as a reference. This probe induces a negligible aerodynamic disturbance by itself, and can detect the perturbations set off by a variety of stems, prongs, or complete probe units which are advanced toward it from various directions.

Most of the systematic tests were performed in a low turbulence flow, and experimental results on mean-velocity perturbations were compared, when possible with those evaluated by a potential flow approach. A few additional tests were made in a high turbulence flow, but they were only intended to detect overall errors in mean velocity and RMS measurements of longitudinal velocity fluctuations.

Naturally, the "rotation" tests performed with only one probe, according to the Hoole and Calvert procedure, led to additional valuable information and some of these findings are reported here.

---

[1] Numbers in brackets designate References at end of paper.

Contributed by the Applied Mechanics Division for publication (without presentation) in the Journal of Applied Mechanics.

Discussion on this paper should be addressed to the Editorial Department, ASME, United Engineering Center, 345 East 47th Street, New York, N. Y. 10017, and will be accepted until January 20th. Discussion received after this date will be returned. Manuscript received by ASME Applied Mechanics Division, July 6, 1970; final revision, December 30, 1970. Paper No. 71-APM-T.

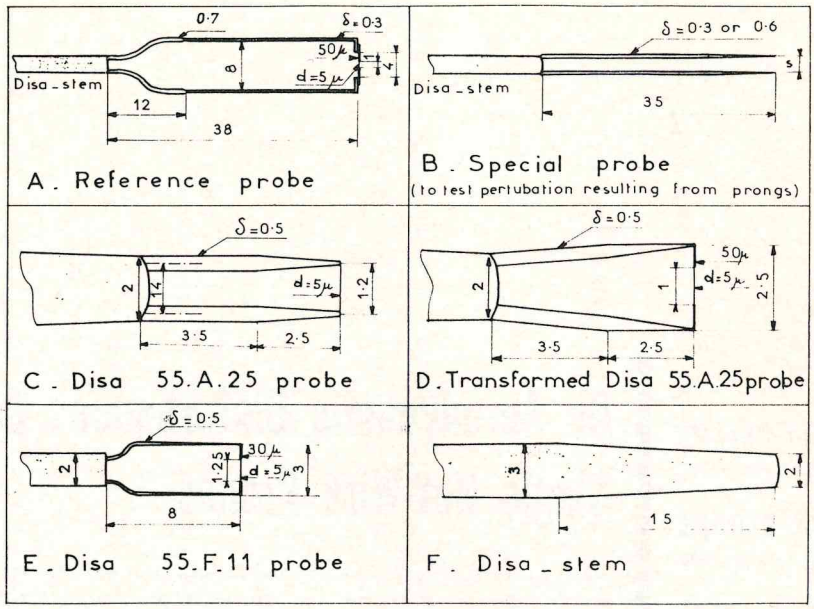


**Fig. 1 Probe configurations (except when mentioned otherwise, all values are given in mm)**

## Experimental Procedure

The experiments were carried out on the axis of a circular jet of air (diameter $a$ = 8 cm) at the downstream location $x/a$ = 0.25 for tests at low turbulence-level ($u'/U$ = 0.9 percent), and at $x/a$ = 14 for tests at high turbulence-level ($u'/U$ = 19 percent). In producing this circular jet of air with a velocity of 7.0 m/s at the given locations (except when otherwise mentioned) a pressure box was equipped with efficient dust filters [Schneider-Poëlman, yellow type] and a contraction design with a ratio of 16 to 1.

The reference probe, Fig. 1($a$), whose efficacy was judged through a global rotation test, Fig. 2, has long and fine prongs embedded in a Disa stem.

The perturbing bodies are as follows:

1 A Disa stem, Fig. 1($f$); also, cylindrical stems of 4 and 2 mm in diameter.

2 A set of special probes, Fig. 1($b$) for testing the perturbation caused only by the prongs, the length of which (35 mm) is such that the perturbation caused by the stem is negligible (cf. Fig. 4).

3 A commercial Disa 55-A-25 probe, Fig. 1($c$), the prongs of which are only 1.2 mm apart, and the wire of which (usually a 5$\mu$ tungsten wire coated with platinum and electrically soldered on the tips of the prongs) extends from one prong to the other.

4 A home-transformed Disa probe, Fig. 1($d$), with an increased prong spacing of 2.5 mm, allowing the hot wire to be far from the prongs; the wire is a Wollaston composition of silver and platinum (10:1), 1 mm in length and 5$\mu$ in diameter.

5 The recent Disa probe 55-F-11, whose prong spacing the manufacturer has increased, Fig. 1($e$).

The probe setups were as follows:

For global rotation tests the probe was mounted on a turntable in such a way that when rotated, the wire always remained along the rotational axis of the turntable and normal to the mean velocity direction, Figs. 2, 3, and 10. Probe location was established by the angle $\alpha$ between the stem axis and the mean velocity direction, with the accuracy of $\alpha$ estimated at about 0.1 deg.

For the test performed with the aid of the reference probe, perturbing bodies were mounted on the turntable, while the reference probe was held with its stem axis normal to the mean flow and with its wire set along the rotational axis of the turntable, Figs. 4–8 and 11. The fine displacements of the perturbing bodies with respect to the reference wire, were obtained by means of a small carriage driven by a micrometer head. The zero separation readings, necessary when the perturbing bodies are prongs, were estimated by observing the prongs and nearby reference wire through a microscope. The accuracy of the separation was estimated to be about 0.01 mm.

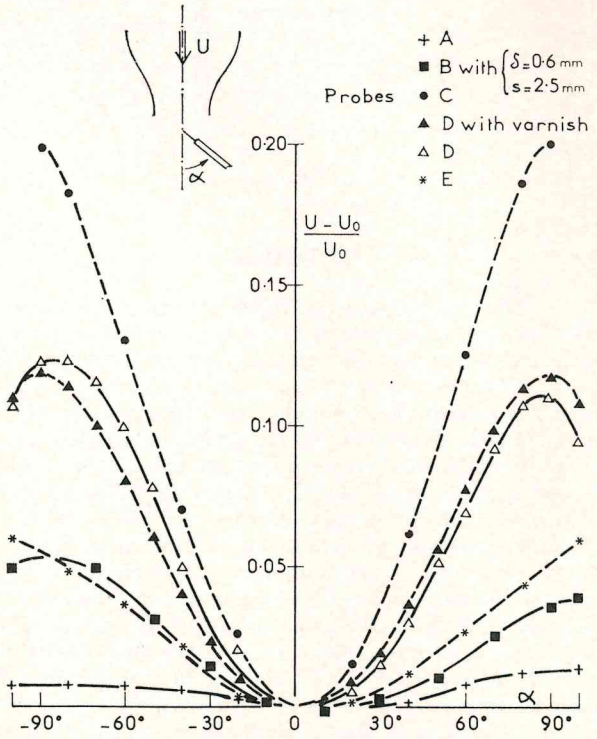


**Fig. 2 Rotation test for probes sketched in Fig. 1**

Operating at a constant current intensity with an average overheated ratio of 0.8, the hot wires, in order to be calibrated, were

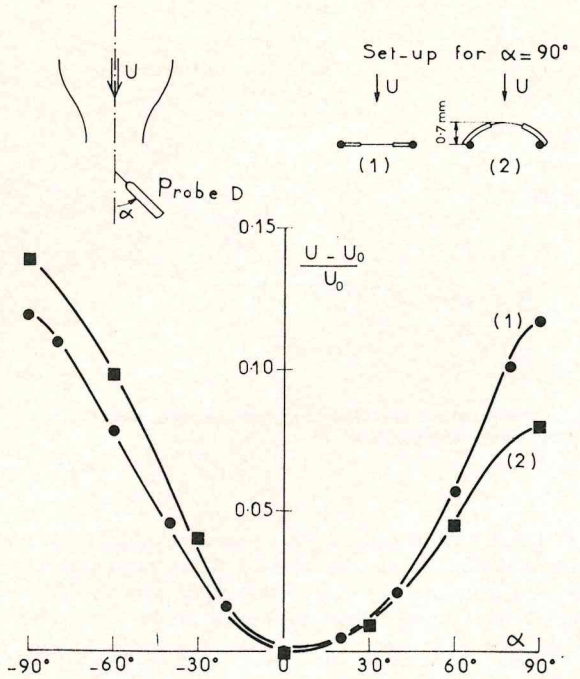


Fig. 3 Rotation test showing effect of wire location with respect to plane of prongs

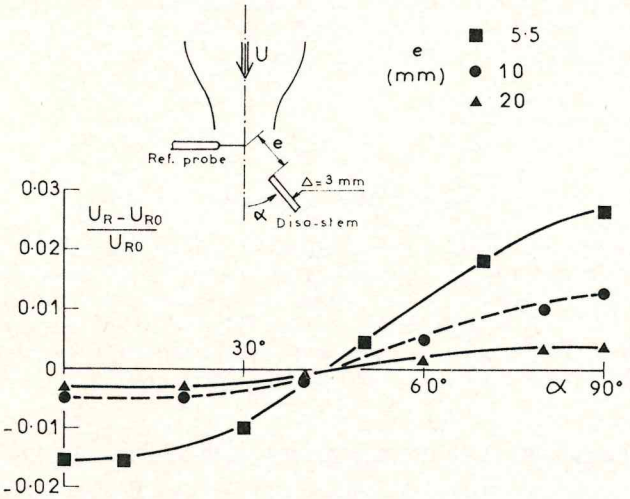


Fig. 4 Response of reference probe in presence of a Disa stem (Δ = 3 mm)

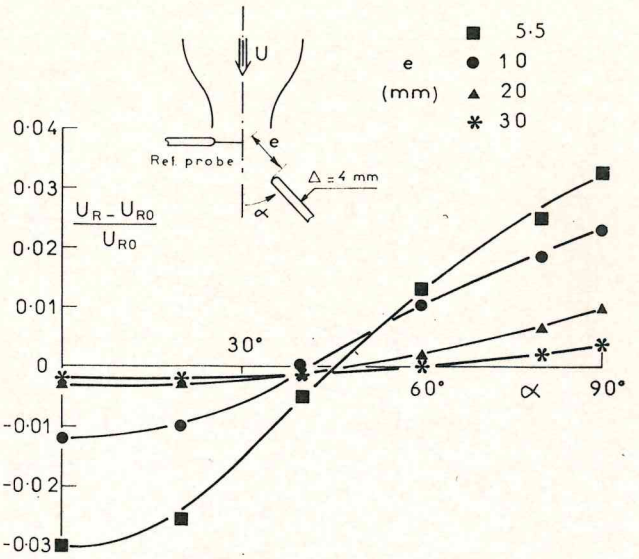


Fig. 5 Response of reference probe in presence of a cylindrical rod (Δ = 4 mm)

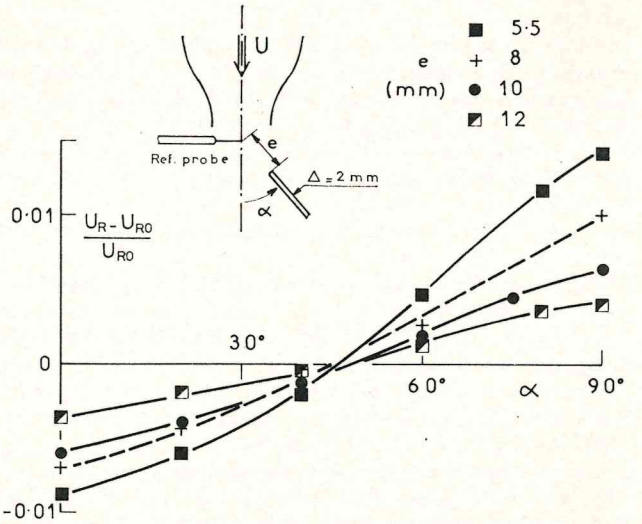


Fig. 6 Response of reference probe in presence of a cylindrical rod (Δ = 2 mm)

placed at $x/a = 0.25$, where turbulent fluctuations are minimal, and the empirical curves of voltage versus velocity (read on a pitot tube) were plotted [14]. The probes that will later be used in global rotation tests were calibrated when their stems were aligned with the mean velocity (i.e., $\alpha = 0$ deg in Fig. 2). Probe A, when later used as a reference probe, was calibrated while situated in its usual position (i.e., with the stem perpendicular to the mean velocity, Fig. 4). The turbulence data, as referred to in the last section, were taken with the use of a Tacussel amplifier [15] with a selected band width of 2 Hz–16 kHz.

Essential notations for velocity values are as follows:

$U_0$, $U$ = mean velocity given by a probe when the angle between the stem axis and the mean velocity is, respectively, 0 and $\alpha$.

$U_{R0}$, $U_R$ = mean velocity given by the reference probe, respectively, in the absence and presence of a perturbing body.

$u'_{R0}$, $u'_R$ = RMS of the longitudinal component of the fluctuating velocity given by the reference probe in the absence and presence of a perturbing body.

## Experimental Results for Low Turbulence Level

The results obtained in the global rotation tests, performed according to the Hoole and Calvert procedure, are indicated in Fig. 2 for all the probes described in Fig. 1. Here the probe geometry clearly appears as a relevant parameter. In particular, the response of the reference probe (Probe A) is almost independent of $\alpha$, the total change observed as $\alpha$ varies from 0 deg to $\pm 90$ deg being less than 1.5 percent. Yet attempts to further reduce this value were not successful, since thinner and longer prongs introduce vibrations.

For the transformed Disa probe (Probe D), tests were repeated after the prongs and the sheath had been coated with a glycerophtalique varnish known as "Loryvolt." Our findings, Fig. 2, revealed that the varnish had almost no effect with respect to $\alpha$

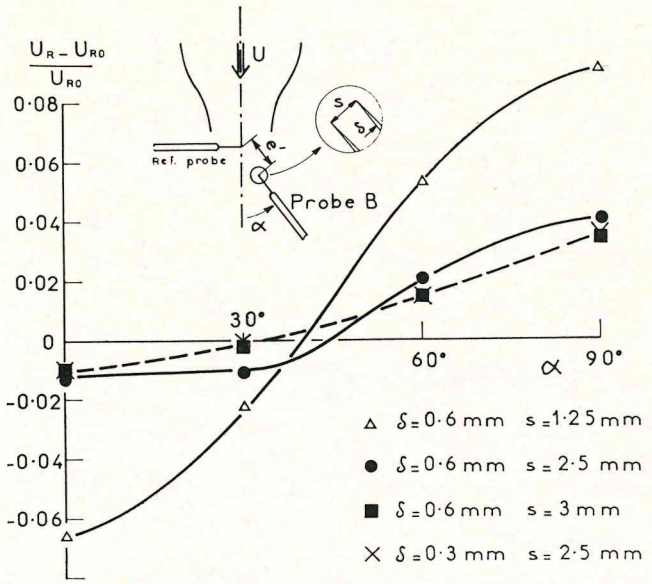


**Fig. 7 Response of reference probe in presence of prongs differing in diameter and spacing; see definitions of $\delta$ and $s$ in Fig. 1(b)**

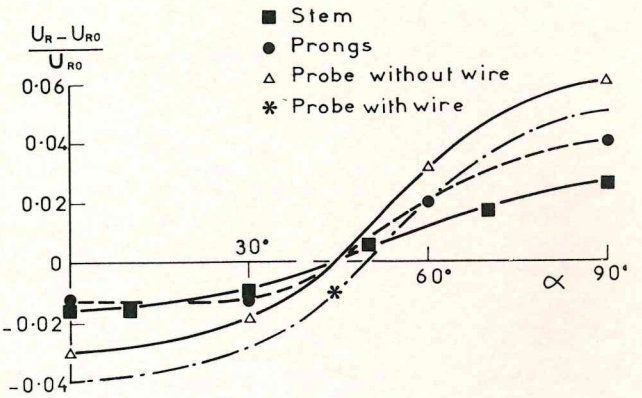


**Fig. 8 Perturbations resulting from stem, prongs, and wire of Probe D, in relative order of magnitude**

and that the hypothesis mentioned in [6, 7], according to which changes in the cooling of the prongs is an important factor of perturbation, does not appear very plausible. Later on, this conclusion will be reconfirmed by other results.

In Fig. 2, in addition to the foregoing findings, a slight asymmetry of the curves with respect to the ordinate axis appeared, which is the result of the wire not being exactly in the plane of the prongs. This nonalignment occurs more frequently with soft-soldered wires (which have a tendency to slide to one side of the prongs) than with electrically soldered wires (which can be kept on the tips of the prongs). Fig. 3 illustrates this point by means of a probe (Probe D) which exaggerates this asymmetry, the result being that greater perturbation is produced when the wire is downstream of the plane of the prongs than when it is upstream, simply because the wakes of the prongs result in a slight velocity increase between them.

The results obtained by using the reference probe begin with Figs. 4–6 which indicate the perturbations caused by a Disa stem, and two cylindrical rods. Here angle $\alpha \approx 45$ deg appears to correspond to a "neutral" direction where the blocking effect of the stem, maximal at $\alpha = 0$ deg, balances the acceleration effect, maximal at $\alpha = \pm 90$ deg. At $\alpha \approx 0$ deg or 90 deg, $(U_R - U_{R0})/U_{R0}$ is observed, from separate logarithmic plots, to vary as to $\Delta^2$ and $e^{-2}$. The preliminary results (for $\alpha \approx 0$ deg) will be resubstantiated in the next section where a less empirical evaluation is given. Finally, the perturbation becomes negligible for $e/\Delta \geq 10$; therefore one can consider that the lengths chosen for the prongs of Probe B are correct.

The perturbation resulting from various prongs is indicated in Fig. 7, where each experimental point is obtained by an extrapolation toward $e' = 0$ of the auxiliary curve $(U_R - U_{R0})/U_{R0}$ versus $e'$, at fixed $\alpha$. Here the parameter $s$ is quite relevant and, from the three values of $s$ used, the resulting perturbation varies roughly as $s^{-2}$ for $\alpha$ close to 0 deg, and as $s^{-1}$ for $\alpha$ close to 90 deg. In addition, the value $\alpha \approx 45$ deg once again corresponds to a "neutral" direction.

The perturbation resulting from complete hot-wire probes is investigated, as before, by extrapolation toward $e' = 0$ of the curve $(U_R - U_{R0})/U_{R0}$ versus $e'$ at fixed $\alpha$. Fig. 8 which corresponds to Probe D demonstrates this situation. Here the sheath effect clearly appears as a slight velocity decrease for any $\alpha$. However, the small value ($\approx -0.9$ percent) generated by the 50 $\mu$-sheath will be negligible for the thinner wires which are usually employed for turbulence investigations.

In Table 1 the results are given for the perturbations created by several complete probes, along with the impartations of the stem and the prongs, and the results of the global rotation tests. From Table 1, three conclusions can be drawn.

1 The total perturbation equals approximately the sum of the separate ones.

2 The perturbation created by the prongs is usually the largest, which explains the acute influence that wire location has with respect to the prongs.

3 Good agreement exists between the total difference

$$\left[\frac{U_R - U_{R0}}{U_{R0}}\right]_{\alpha = 0 \text{ deg}}^{\alpha = 90 \text{ deg}}$$

as displayed by the reference probe and the values of

$$\left[\frac{U - U_0}{U_0}\right]_{\alpha = 0 \text{ deg}}^{\alpha = 90 \text{ deg}}$$

as observed in the global rotation test. Therefore, our results show that a modification of the flow pattern by the probe and not a modification of the prongs temperature by the flow, accounts for the probe-direction effect, since no contact exists, at any time, between the probe under investigation and the reference probe which is moreover in the upstream position.

## Evaluations by an Irrotational Flow, Inviscid Fluid, Approach

**Stem at $\alpha = 0$ deg.** An axisymmetric flow past the stem at $\alpha = 0$ deg is obtained from a uniform stream $U_\infty$ with a point source of strength $4\pi S$ at origin 0, Fig. 9(*a*), where $S$ is related to the asymptotic stem diameter $\Delta$ by $S = \frac{\Delta^2}{16} U_\infty$. The result is that the decrement from $U_\infty$ of the longitudinal component of the velocity at point $M$, on the hot wire of reference, is

$$\frac{U_M - U_\infty}{U_\infty} = -\frac{\Delta^2}{16} \frac{e + |x_A|}{[y^2 + (e + |x_A|)^2]^{3/2}} \qquad (1)$$

where $x_A$ is the abscissa of the stagnation point, related to $\Delta$ by $x_A = -\Delta/4$. A Disa stem with an abscissa of $x_A = -0.75$ mm leads moreover to $BB' = 2\sqrt{2}|x_A| \simeq 2.1$ mm which fits the dimensions given in Fig. 1(*f*). For the circular rods of 2 and 4 mm dia, $x_A = -0.6$ and $-1.2$ mm were used, respectively, the average between $\Delta$ and $BB'$ being close to the real diameters. Since the velocity decrement in equation (1) is quite independent of $y$ for the values of $e$ used here (a 0.01 percent variation existing between one end and the middle of the wire for $e = 5.5$ mm), the values of equation (1) for $y = 0$ can be directly compared to the experimental results in Figs. 4–6:

**Table 1 Perturbation due to different parts of Probes C, D, and E—comparison with global rotation test**

| PROBE: C | | $\frac{U_R - U_{R0}}{U_{R0}}_{\alpha=0\text{ deg}}$ | $\frac{U_R - U_{R0}}{U_{R0}}_{\alpha=90\text{ deg}}$ | $\left[\frac{U_R - U_{R0}}{U_{R0}}\right]_{\alpha=0\text{ deg}}^{\alpha=90\text{ deg}}$ | $\left[\frac{U - U_0}{U_0}\right]_{\alpha=0\text{ deg}}^{\alpha=90\text{ deg}}$ |
|---|---|---|---|---|---|
| Stem | | −1.5% | 2.6% | 4.1% | |
| Prongs | | −6.6% | 9.0% | 15.6% | |
| Whole probe | Add | −8.1% | 11.6% | 19.7% | |
| | Exp | −9.1% | 10.5% | 19.6% | 20.0% |

| PROBE: D | | $\frac{U_R - U_{R0}}{U_{R0}}_{\alpha=0\text{ deg}}$ | $\frac{U_R - U_{R0}}{U_{R0}}_{\alpha=90\text{ deg}}$ | $\left[\frac{U_R - U_{R0}}{U_{R0}}\right]_{\alpha=0\text{ deg}}^{\alpha=90\text{ deg}}$ | $\left[\frac{U - U_0}{U_0}\right]_{\alpha=0\text{ deg}}^{\alpha=90\text{ deg}}$ |
|---|---|---|---|---|---|
| Stem | | −1.5% | 2.6% | 4.1% | |
| Prongs | | −1.25% | 4.0% | 5.25% | |
| Wire-sheath (50 $\mu$) | | −0.9% | −0.9% | | |
| Whole probe | Add | −3.65% | 5.7% | 9.35% | |
| | Exp | −3.9% | 5.1% | 9.0% | 11.0% |

| PROBE: E | | $\frac{U_R - U_{R0}}{U_{R0}}_{\alpha=0\text{ deg}}$ | $\frac{U_R - U_{R0}}{U_{R0}}_{\alpha=90\text{ deg}}$ | $\left[\frac{U_R - U_{R0}}{U_{R0}}\right]_{\alpha=0\text{ deg}}^{\alpha=90\text{ deg}}$ | $\left[\frac{U - U_0}{U_0}\right]_{\alpha=0\text{ deg}}^{\alpha=90\text{ deg}}$ |
|---|---|---|---|---|---|
| Stem | | −0.7% | 1.0% | 1.7% | |
| Prongs | | −1.05% | 3.8% | 4.85% | |
| Wire-sheath (30 $\mu$) | | −0.65% | −0.65% | | |
| Whole probe | Add | −2.4% | 4.15% | 6.55% | |
| | Exp | −3.1% | 3.6% | 6.7% | 6.0% |

**Table 2 Perturbation due to stem at $\alpha$ = 0 deg—comparison between evaluation and experiment**

| $e$ (mm) | Disa stem ($\Delta$ = 3 mm) | | 4 mm circular rod | | 2 mm circular rod | |
|---|---|---|---|---|---|---|
| | $\frac{U - U_\infty}{U_\infty}$ | $\frac{U_R - U_{R0}}{U_{R0}}$ | $\frac{U - U_\infty}{U_\infty}$ | $\frac{U_R - U_{R0}}{U_{R0}}$ | $\frac{U - U_\infty}{U_\infty}$ | $\frac{U_R - U_{R0}}{U_{R0}}$ |
| 5.5 | −1.44% | −1.5% | −3.20% | −3.0% | −0.97% | −0.9% |
| 8 | ... | ... | ... | ... | −0.49% | −0.7% |
| 10 | −0.49% | −0.5% | −1.15% | −1.25% | −0.32% | −0.6% |
| 12 | ... | ... | ... | ... | −0.23% | −0.35% |
| 20 | −0.13% | −0.3% | −0.32% | −0.3% | ... | ... |
| 30 | −0.06% | ≃0 | −0.15% | −0.2% | ... | ... |

$$\frac{U - U_\infty}{U_\infty} = -\frac{\Delta^2}{16}\frac{1}{(e + |x_A|)^2} \tag{2}$$

Table 2 shows a very satisfactory agreement.

**Prongs at $\alpha$ = 0 deg.** As the prongs are linearly tapered along their last 3 mm, an axisymmetric flow past one of them, at $\alpha$ = 0 deg, is obtained from a uniform stream $U_\infty$, and a set of six sources of equal strength $4\pi S'$, equally spaced (0.5 mm) on the $x$-axis at points of abscissa $x_1, x_2, \ldots, x_6$, Fig. 9($b$). Here $S'$ is related to the asymptotic prong diameter $\delta$ by $S' = \frac{\delta^2}{96} U_\infty$. The longitudinal velocity decrement at point $M$, on the hot wire of reference is now

$$\frac{U_M - U_\infty}{U_\infty} = \frac{\delta^2}{96}\sum_{i=1}^{6}\frac{x_A - x_i}{[y^2 + (x_A - x_i)^2]^{3/2}} \tag{3}$$

and the abscissa of the stagnation point is approximately

$$x_A \simeq x_1 - \frac{\delta}{4\sqrt{6}}$$

With Probe C, which exhibited the highest level of perturbation, the decrements were −16 percent, −0.96 percent, and − 0.43 percent at points C, I, and D, respectively, Fig. 9($b$). Since the decrement is small from the middle to the end of the wire (part I-D), the disturbance of the second prong will simply be added to that of the first prong. And since the decrement varies slightly along the entire wire, any change in the temperature profile along the wire, due to a nonuniform velocity field [16, section 27] will be left out. Thus the observed aerodynamic perturbation resulting from the wire is

$$\frac{\bar{U} - U_\infty}{U_\infty} = 2\frac{\delta^2}{96}\frac{1}{2l}\int_{y_1}^{y_1+2l}\sum_{i=1}^{6}\frac{(x_A - x_i)dy}{[y^2 + (x_A - x_i)^2]^{3/2}} \tag{4}$$

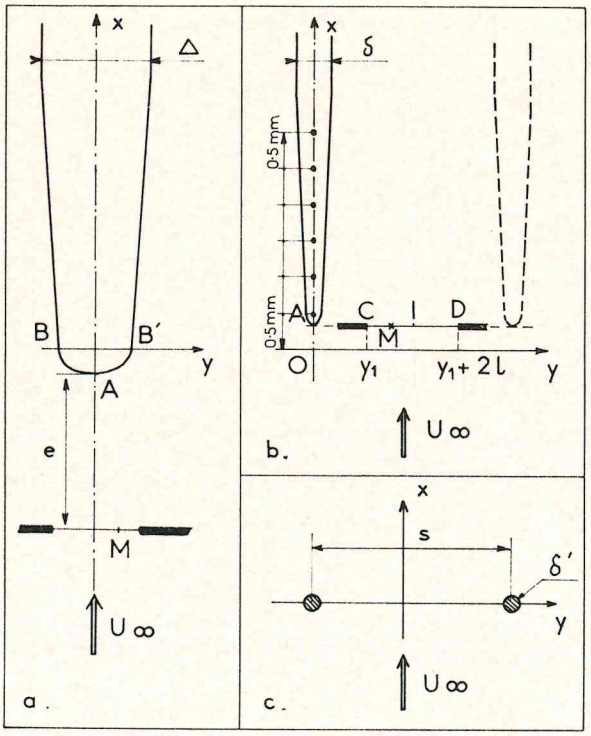


**Fig. 9(a) Flow past a stem at $\alpha = 0$ deg; (b) flow past a prong at $\alpha = 0$ deg; and (c) flow past prongs at $\alpha = 90$ deg**

**Table 3 Perturbation due to prongs at $\alpha = 0$ deg—comparison between evaluation and experiment**

| Prongs | $\frac{\bar{U} - U_\infty}{U_\infty}$ | $\frac{U_R - U_{R0}}{U_{R0}}$ |
|---|---|---|
| $\delta = 0.6$ mm<br>$s = 1.2$ mm | −3.7% | −6.6% |
| $\delta = 0.6$ mm<br>$s = 2.5$ mm | −0.78% | −1.2% |
| $\delta = 0.6$ mm<br>$s = 3$ mm | −0.60% | −1.05% |

Numerical values are given in Table 3, and once again satisfactory agreement can be seen to exist with the experimental results.

**Prongs at $\alpha = 90$ deg.** Although of finite length, the prongs can be considered as two infinite cylinders normal to the flow. In effect, we have experimentally observed that a hot wire soldered between the prongs of Probe C, located at $\alpha = -90$ deg, displays only a 1.1 percent absolute increase in perturbation when Probe B, with the same prong spacing ($s = 1.2$ mm, $\delta = 0.6$ mm) is aligned with it from the direction $\alpha = +90$ deg.

As a result the corresponding plane flow field is simply obtained from a uniform flow and two sources separated by a distance $s$, Fig. 9(c). Thus the increment in the longitudinal velocity component at the point $M$ on the reference wire is

$$\frac{U_M - U_\infty}{U_\infty} = 2\left(\frac{\delta'}{2}\right)^2 \frac{y^2 + \left(\frac{s}{2}\right)^2}{\left[y^2 - \left(\frac{s}{2}\right)^2\right]^2} \tag{5}$$

$\delta'$ equaling approximately the prong diameter at the position where the wire is soldered.

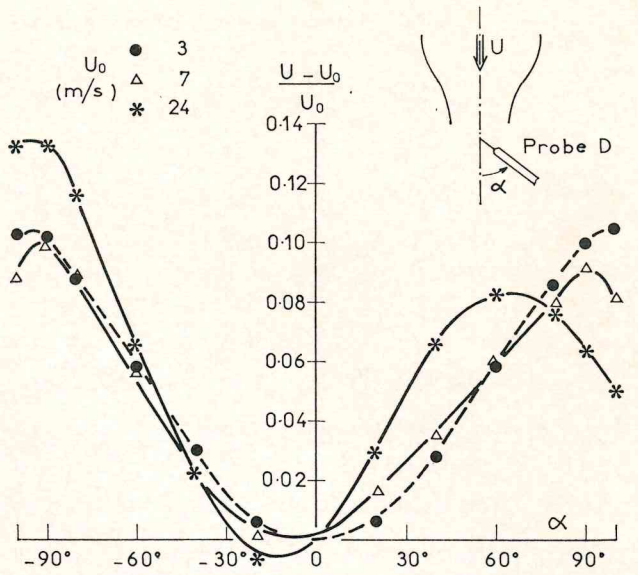


**Fig. 10 Rotation test for different velocities**

**Table 4 Perturbation due to prongs at $\alpha = 90$ deg—comparison between evaluation and experiment**

| Prongs | $\frac{\bar{U} - U_\infty}{U_\infty}$ | $\frac{\tilde{U} - U_\infty}{U_\infty}$ | $\frac{U_R - U_{R0}}{U_{R0}}$ |
|---|---|---|---|
| $\delta = 0.6$ mm<br>$s = 1.2$ mm | 18% | 9.8% | 9.0% |
| $\delta = 0.6$ mm<br>$s = 2.5$ mm | 3.5% | 3.6% | 4.1% |
| $\delta = 0.6$ mm<br>$s = 3$ mm | 2.4% | | 3.8% |

As equation (5) strongly depends on $y$ in some cases, two average velocities are evaluated: an approximate one $(\bar{U} - U_\infty)/U_\infty$, for which the change in the temperature profile, along the wire, is neglected and a more elaborate one $(\tilde{U} - U_\infty)/U_\infty$, for which this change is taken into account (see the Appendix).

Numerical values are given in Table 4, for the smallest prong spacing ($s = 1.2$ mm). Here, the two averages differ by a factor of 2, and the experimental results $(U_R - U_{R0})/U_{R0}$, found in Fig. 7, are in close agreement with the $(\tilde{U} - U_\infty)/U_\infty$ values.

However, one should not ask too much of this irrotational flow approach; as an example, the asymmetrical location of the wire with respect to the plane of the prongs could not have been adequately evaluated.

## A Few Experimental Results at a High Turbulence Level

In preliminary investigations in high turbulence level, a few global rotation tests were carried out for Probe D at different jet-velocity values: 3, 7, and 24 m/s. The results, Fig. 10, show, in spite of the asymmetry which appears at high velocity, that the overall relative perturbation is almost unaffected. This finding is in agreement with an irrotational flow inviscid fluid approach, since the absolute value of the velocity does not enter into these evaluations.

The reference probe was then located at $x/a = 14$ where $u'_{R0}/U_{R0} = 19$ percent and $U_{R0} = 7$ m/s. The mean and fluctuation velocity readings transmitted by the reference probe, when Probe D was advanced toward it from various directions, are given in Fig. 11. As expected, $u'_R$ and $U_R$ similarly depend

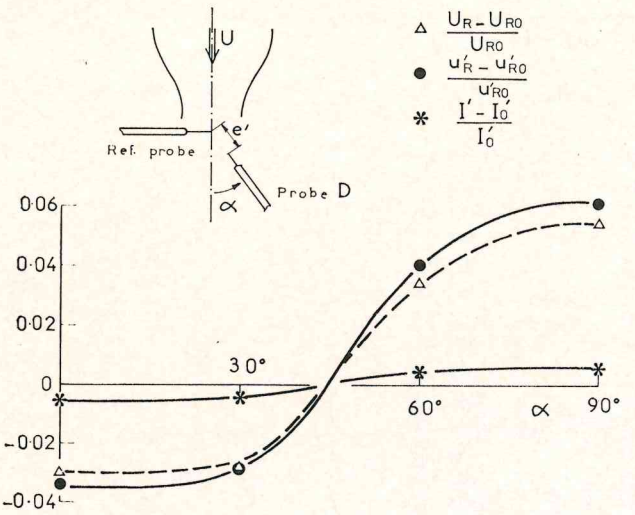


**Fig. 11 Mean and fluctuating velocity readings of the reference probe in the presence of Probe D**

on $\alpha$; the result being that the turbulence intensity $I' = \frac{u'_R}{U_R}$ is almost free of error. Concerning $U_R$, one can notice that the perturbations at $\alpha \approx 0$ deg and $\alpha \approx 90$ deg are slightly smaller that those observed in low turbulence flow, which is simply due to the averaging effect of the instantaneous values of $U_R$ which correspond to a larger $\alpha$ spread.

## Conclusion

Discrepancies obtained during airflow investigations where single hot-wire probes were oriented by their axis to the flow, the wires themselves being kept normal to the flow, can be accounted for by the aerodynamic perturbation induced by the probe, and not by a differential rate of prong cooling. This point of view is jointly supported by experiments carried out with an auxiliary reference probe located upstream from the probes under investigation, and by evaluations of the irrotational flow pattern.

There is a velocity decrement when a probe is aligned with the flow [$(U_R - U_{R0})/U_{R0} < 0$ at $\alpha \approx 0$ deg], and a velocity increment when a probe is normal to the flow [$(U_R - U_{R0})/U_{R0} > 0$ at $\alpha \approx 90$ deg]. Furthermore, a direction which is neutral in aerodynamic effect appears for $\alpha \approx 45$ deg.

The perturbation resulting from the prongs is larger than that created by the stem and varies approximately as the inverse of the prong spacing at $\alpha = 90$ deg, and as the inverse square of the prong spacing at $\alpha = 0$ deg.

The perturbation resulting from a stem at $\alpha \approx 0$ deg or $\alpha \approx 90$ deg varies approximately as the square of the stem diameter and as the inverse square of the distance between the wire and the stem.

From a practical point of view, a reduced level of perturbation, 2.5 percent in absolute value, for any $\alpha$, can be obtained, for example, by using the following dimensions:

| | |
|---|---|
| Stem Diameter: | 3 mm |
| Prongs Length: | 20 mm |
| Prongs Diameter: | 0.6 mm |
| Prongs Spacing: | 6 mm |

Wollaston sheaths, at least those less than 50 $\mu$, induce negligible perturbation (less than 0.9 percent), and thus wires can be chosen according to the unsteady response required by the problem under investigation.

## Acknowledgments

We are grateful to W. M. Howdon, presently Lecturer at the Ecole Centrale, for his patience and most useful help in the editing of this article. We also thank Prof. J. Mathieu for his many valuable suggestions.

## References

1 Webster, C. A. G., "A Note on the Sensitivity to Yaw of a Hot-Wire Anemometer," *Journal of Fluid Mechanics*, Vol. 13, 1962, pp. 307–312.

2 Tritton, D. J., "Note on the Effect of a Nearby Obstacle on Turbulence Intensity in a Boundary Layer," *Journal of Fluid Mechanics*, Vol. 28, 1967, pp. 433–437.

3 Kovasznay, L. S. G., "Hot-Wire Investigation of the Wake Behind Cylinders at Low Reynolds Numbers," *Proceedings of the Royal Society*, Series A, Vol. 198, 1949, pp. 174–190.

4 Berger, E., "Die Bestimmung der hydrodynamischen Grossen einer Karmanschen Wirbelstrasse aus Hitzdrahtmessungen bei kleinen Reynoldsschen Zahlen," *Zeitschrift für Flugwissenschaften*, Vol. 2, 1964, pp. 41–59.

5 Hoole, B. J., and Calvert, J. R., "The Use of a Hot-Wire Anemometer in Turbulent Flow," *Journal of the Royal Aeronautical Society*, Vol. 71, 1967, pp. 511–513.

6 Eyre, D., "End Conduction and Angle of Incidence Effects in Single Hot-Wire Anemometer Probes," TRG Report 1521-W, United Kingdom Atomic Energy Authority, 1967.

7 van Thinh, N., "Sur la mesure de la vitesse dans un écoulement turbulent par anémométrie à fil chaud au voisinage d'une paroi lisse," *Compte Rendu de l'Academie des Sciences*, Paris, Series A, Vol. 264, 1967, pp. 1150–1152.

8 Gilmore, D. C., "The Probe Interference Effect of Hot-Wire Anemometers," TN 67-3, Mechanical Engineering Research Laboratory, McGill University, 1967.

9 Mathieu, J., and Tailland, A , private communication.

10 Florent, P., and Thiolet, G., "Importance de l'orientation d'un support de sonde à fil chaud par rapport à une paroi sur la détermination des vitesses moyennes dans une couche limite turbulente," University of Poitiers (not published).

11 Dahm, M., and Rasmussen, C. G., "Effect of Wire Mounting System on Hot-Wire Probe Characteristics," Disa Information, No. 7, 1969, pp. 19–24.

12 Friehe, C. A., and Schwarz, W. H., "Deviations From the Cosine Law for Yawed Cylindrical Anemometer Sensors," JOURNAL OF APPLIED MECHANICS, Vol. 35, TRANS. ASME, Vol. 90, Series E, 1968, pp. 655–662.

13 Champagne, F. H., Sleicher, C. A., and Wehrmann, O. H., "Turbulence Measurements With Inclined Hot Wires (Part 1)," *Journal of Fluid Mechanics*, Vol. 28, 1967, pp. 153–175.

14 Comte-Bellot, G., and Mathieu, J., "Sur la determination expérimentale des coefficients de sensibilité aux fluctuations de vitesse et de température des anémomètres à fil chaud," *Compte Rendu de l'Academie des Sciences*, Paris, Vol. 246, 1958, pp. 3219–3222.

15 Tacussel, J., Mathieu, J., and Ailloud, M., "Chaine amplificatrice pour anémomètre à fil chaud," *Compte Rendu de l'Academie des Sciences*, Paris, Vol. 252, 1961, pp. 3532–3534.

16 Corrsin, S., "Turbulence: Experimental Methods," *Handbuch der Physik*, Vol. VIII—2, Springer-Verlag, 1963, pp. 523–590.

## APPENDIX

The temperature profile for a wire of finite length as derived by Corrsin [16] is given by the differential equation:

$$\frac{d^2}{dy^2}(\theta - \theta_a) - \frac{4\psi R_a}{\pi d^2 k}(A + B\sqrt{U} - I^2)(\theta - \theta_a) = -\frac{4R_a I^2}{\pi d^2 k} \quad (6)$$

and the boundary conditions $\theta - \theta_a = 0$ for $y = \pm l$. The notations are: $\theta$, the wire-temperature at point $y$; $\theta_a$, the ambient temperature; $A$ and $B$, the "constants" in King's law; $I$, the current intensity; $R_a$, the wire resistance at temperature $\theta_a$; $d$, the wire diameter; $k$, the thermal conductivity of the wire material; $\psi$, the temperature coefficient in a linear dependence of the wire material resistivity on temperature.

Equation (6) is numerically solved by the Runge-Kutta 4 method for a nonuniform velocity profile and for a uniform one. The mean temperature of the wire is then computed where $\tilde{\theta}$ stands for a nonuniform velocity profile, and $\bar{\theta}$ stands for a

**Table 5 Temperature distribution along a wire, in deg C: (1)—uniform velocity profile; (2)—velocity profile according to equation (5)**

| $y/e$ | $\theta - \theta_a$ (1) | $\theta - \theta_a$ (2) |
|---|---|---|
| 0 | 315.48 | 315.00 |
| 0.05 | 314.63 | 314.14 |
| 0.1 | 312.07 | 311.59 |
| 0.15 | 307.81 | 307.33 |
| 0.2 | 301.86 | 301.39 |
| 0.25 | 294.24 | 293.78 |
| 0.3 | 284.96 | 284.51 |
| 0.35 | 274.04 | 273.61 |
| 0.4 | 261.51 | 261.10 |
| 0.45 | 247.40 | 247.01 |
| 0.5 | 231.75 | 231.38 |
| 0.55 | 214.59 | 214.25 |
| 0.6 | 195.95 | 195.64 |
| 0.65 | 175.90 | 175.62 |
| 0.7 | 154.46 | 154.22 |
| 0.75 | 131.70 | 131.49 |
| 0.8 | 107.67 | 107.50 |
| 0.85 | 82.42 | 82.29 |
| 0.9 | 56.02 | 55.93 |
| 0.95 | 28.52 | 28.48 |
| 1 | 0.00 | 0.00 |

uniform one. Finally, the difference $\tilde{\theta} - \bar{\theta}$ is transformed into a velocity difference $(\tilde{U} - U_\infty)/U_\infty$ (note that $\bar{U} = U_\infty$) by means of the linear relations:

$$\tilde{R} - \bar{R} = \psi R_a(\tilde{\theta} - \bar{\theta})$$

and

$$\tilde{U} - U_\infty \approx -\frac{2I^2}{B}\sqrt{U_\infty}\,\frac{R_a}{(\bar{R} - R_a)}\,(\tilde{R} - \bar{R})$$

where $\tilde{R}$ and $\bar{R}$ are the mean resistances in the two cases.

Table 5 gives a few values of $\tilde{\theta}$ and $\bar{\theta}$ for a Disa 55-A-25 probe and the nonuniform velocity profile given by equation (5) [$\delta' = 0.20$ mm, $U_\infty = 7$ m/s, $y = 0.5$ mm, $s = 1.2$ mm, $d = 5\ \mu$, $I = 65 \times 10^{-3}$ amp, $(\bar{R} - R_a)/R_a = 0.8$, $R_a = 5$ ohms, $\psi = 0.00366\ d^{\circ -1}$, $k = 0.7$ watt $\times$ cm$^{-1} \times d^{-1}$, $B = 0.68 \times 10^{-4} \times$ amp$^2 \times$ cm$^{-1/2} \times s^{-1/2}$, $A = 1.2 \times 10^{-3}$ amp$^2$].

*Reprinted from the December 1971*
*Journal of Applied Mechanics*